AJNR

Dynamic CT of the laterosellar extradural venous spaces.

J F Bonneville, F Cattin, A Racle, M Bouchareb, D Boulard, P Potelon and Y S Tang

AJNR Am J Neuroradiol 1989, 10 (3) 535-542
http://www.ajnr.org/content/10/3/535

Dynamic CT of the Laterosellar Extradural Venous Spaces

J. F. Bonneville[1]
F. Cattin
A. Racle
M. Bouchareb
D. Boulard
P. Potelon
Y. S. Tang

We evaluated the ability of dynamic CT scanning to accurately demonstrate the laterosellar extradural venous spaces. Careful examination of 680 consecutive patients with this technique has permitted us to describe four main venous groups: the veins of the lateral wall (present in 98% of cases), the vein of the inferolateral group located beneath cranial nerve VI (present in 92% of cases), the medial vein located between the internal carotid artery and the pituitary gland (present in 20–30% of cases), and the vein of the carotid sulcus located between the intracavernous internal carotid artery and the lateral wall of the sphenoid bone (present in 65% of cases). The vein of the carotid sulcus is absent only when the internal carotid artery lies close to the sphenoid bone. In 12 patients with suspected cavernous sinus invasion, dynamic CT scanning demonstrated obliteration of the vein of the carotid sulcus. In five patients with huge tumors of the temporal region, dynamic CT scanning of the cavernous sinus permitted demonstration of normal laterosellar extradural venous spaces, thus permitting exclusion of intracavernous sinus invasion.

We believe dynamic CT is the imaging technique best suited for studying the laterosellar extradural venous spaces. Its spatial resolution and dynamic capacity make it superior to MR, and it should be the first procedure when invasion of the cavernous sinus by a pituitary tumor is suspected.

There is controversy and confusion about the exact nature of the parasellar venous spaces. The classical description is of a blood-filled, trabeculated channel completely surrounding the internal carotid artery; other theories maintain that the plexus is composed of various-sized veins [1–12]. Dynamic CT scanning is able to clarify the anatomy in this area. In the case of a cavernous sinus tumor, such as cavernous sinus invasion by pituitary adenoma, the evaluation of the laterosellar veins can be used in diagnosis. We report our results in the examination of the cavernous sinuses with dynamic CT scanning in 680 patients.

Materials and Methods

Since January 1982, 2200 patients with suspected pituitary lesions have been examined by dynamic CT scanning to demonstrate the pituitary tuft and pituitary enhancement [13, 14]. The last 680 of these patients have been specifically examined for demonstration of the cavernous sinus. All dynamic scans of the cavernous sinus were obtained on a GE CT/T 9800 scanner. The patients were placed in the prone position with the head hyperextended. A preinfusion coronal CT scan at the midsellar level was obtained first. In 25 patients, the dynamic coronal CT scan was correlated with the dynamic axial scan at the sellar level. Eighty milliliters of 32% iodinated contrast medium (25 g iodine) pushed with 30 ml of saline solution were mechanically injected at 15 ml/sec through a 16-gauge needle in an arm vein. Dynamic coronal CT scans were obtained during and just after injection (Fig. 1). A section thickness of 1.5 mm and scan time of 2 sec were used at 200 mA and 120 kVp. The first three cuts after the bolus were reconstructed with a special algorithm for bone detail and displayed in the black bone mode (Fig. 2). The maximum surface dose for eight scans is approximately 20 rad (0.2 Gy).

Received April 14, 1988; accepted after revision September 27, 1988.

Presented at the annual meeting of the American Society of Neuroradiology, New York City, May 1987.

[1] All authors: Department of Neuroradiology, University Hospital of Besançon, 25000 Besançon, France. Address reprint requests to J. F. Bonneville.

AJNR **10:535–542, May/June 1989**
0195–6108/89/1003–0535

Results

Visualization of laterosellar veins was obtained in all patients; however, it was considered poor in 10 patients because of either cardiac failure or technical problems. Therefore, in 670 patients, opacification of the parasellar venous plexus was considered good or excellent.

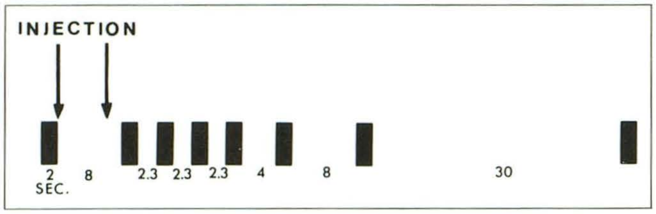

Fig. 1.—Pre- and postinjection intervals between scans. Each scan is represented by black bar.

Normal

Optimal enhancement of the laterosellar veins occurs 5 sec after optimal enhancement of the internal carotid artery. Ten seconds later, the cavernous sinus appears homogeneous, and individualization of the laterosellar veins is not possible because of delayed enhancement of the tiny venous network surrounding the intracavernous internal carotid artery, the intracavernous cranial nerves, and the large laterosellar veins described below. Laterosellar veins are always asymmetric in size and location, while the intracavernous cranial nerves are symmetric. True venous cavernous sinus—that is, a large blood-filled channel extending from the lateral wall of the cavernous sinus to its medial aspect and totally surrounding the intracavernous internal carotid artery and intracavernous cranial nerves—was seen in only four patients (Fig. 3). In all other patients, the laterosellar veins could be divided into five groups: (1) the veins of the lateral wall of the cavernous sinus

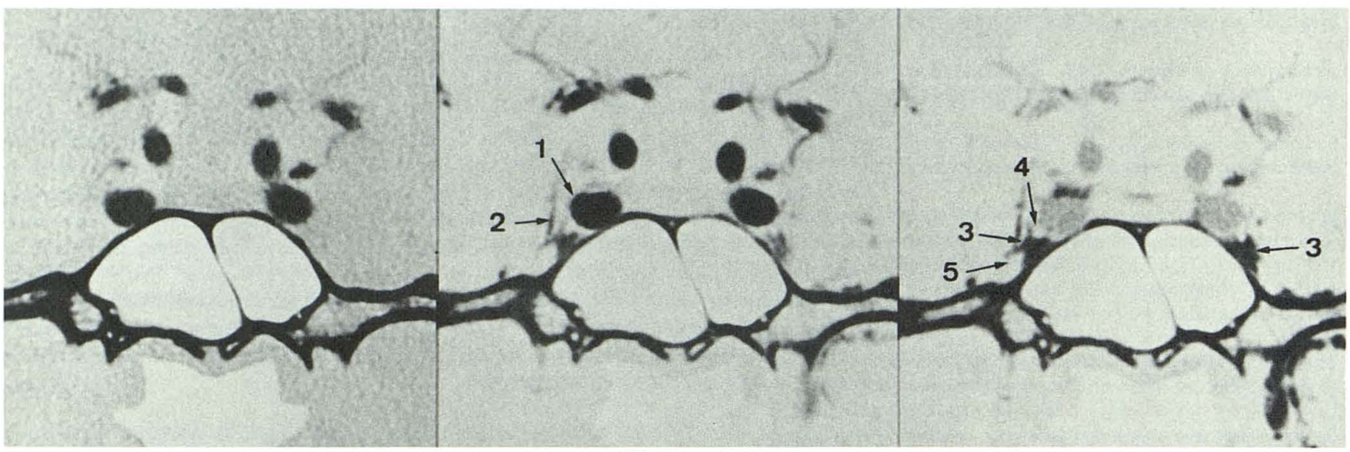

Fig. 2.—Coronal dynamic CT study for demonstrating laterosellar extradural venous spaces. Slices are reconstructed with special algorithm for bone detail. Then, image contrast is reversed. Optimal enhancement of venous spaces occurs 5 sec after visualization of internal carotid arteries. 1 = intracavernous internal carotid artery; 2 = veins of lateral wall of cavernous sinus; 3 = H-like inferolateral venous group; 4 = abducens nerve (VI); 5 = ophthalmic nerve (V_1).

Fig. 3.—Sequential dynamic CT scans. On left, opacification of "true" cavernous sinus surrounds superior, lateral, and inferior aspects of intracavernous internal carotid artery. Detail of intracavernous cranial nerves is exquisite (*arrows*).

(98%), (2) the inferolateral venous group (92%), (3) the vein of the carotid sulcus (65%), (4) the medial vein (20–30%), and (5) the pericarotid plexus (Fig. 4).

Veins of the lateral wall of the cavernous sinus.—The prevalence of these veins is quite constant but they vary in shape and size. In coronal section, these veins generally appear as small and either round, oval, or—more rarely—linear vascular structures partially delineating the lateral wall of the cavernous sinus (Fig. 5). Intracavernous cranial nerves, although in contact with the veins of the lateral wall, do not imprint on the veins.

Inferolateral venous group.—This quite constant venous group (92%) has been described by Daniels et al. [15]. In coronal section, the inferolateral venous group is demonstrated below the intracavernous carotid artery and abducens nerve, which consequently is well demonstrated (Figs. 2 and 6). In axial section, the sagittal orientation of these veins is clearly seen. This group of veins is frequently close to the veins of the lateral wall laterally and to the vein of the carotid sulcus superiorly (Figs. 6–9). The inferolateral venous group is usually bilateral but asymmetric.

Vein of the carotid sulcus.—This vein is located between the intracavernous internal carotid artery and the carotid sulcus of the sphenoid bone (Figs. 6 and 7). The vein of the carotid sulcus can communicate freely with the inferolateral venous group inferiorly and the medial vein superiorly (Fig. 8). When there is a deep carotid sulcus on the lateral wall of the sphenoid bone, the vein of the carotid sulcus is absent or very thin; when thin, the vein is seen later (e.g., 10 sec after optimal enhancement of the internal carotid artery). The vein of the carotid sulcus is absent in those 35% of cases in which

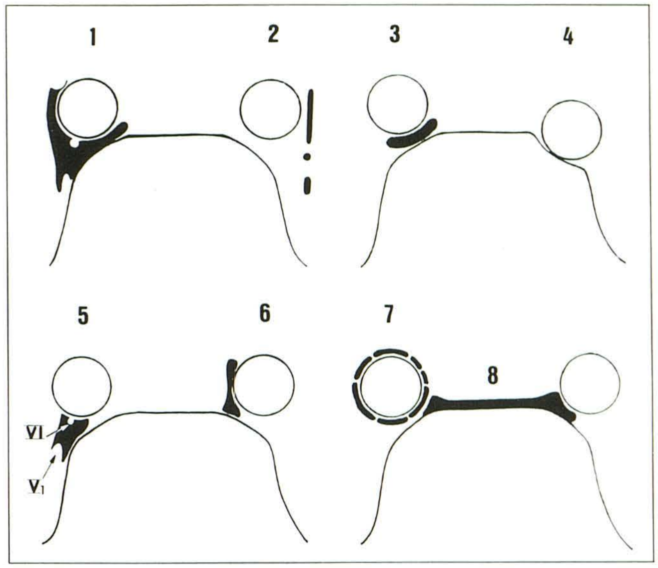

Fig. 4.—Schematic drawing of different patterns of laterosellar extradural venous spaces.
***1*, True cavernous sinus.**
***2*, Veins of lateral wall of cavernous sinus.**
***3*, Vein of carotid sulcus, situated between intracavernous internal carotid artery and sphenoid bone.**
***4*, Absence of vein of carotid sulcus, when intracavernous internal carotid artery is in close contact with sphenoid bone.**
***5*, Inferolateral venous group delineating abducens nerve (VI) and ophthalmic nerve (V_1).**
***6*, Medial vein situated between intracavernous internal carotid artery and pituitary gland.**
***7*, Pericarotid plexus.**
***8*, Inferior intercavernous sinus.**

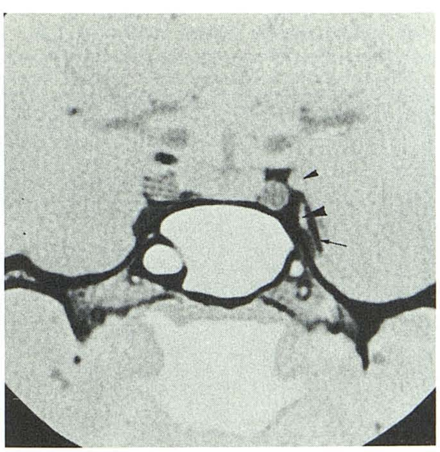

Fig. 5.—Linear vein of lateral wall of cavernous sinus on left (*arrow*). Note imprint of oculomotor nerve (*small arrowhead*) and ophthalmic nerve (*large arrowhead*).

Fig. 6.—Large bilateral veins of carotid sulcus communicate with inferolateral venous group. On right, abducens nerve is well delineated (*arrow*).

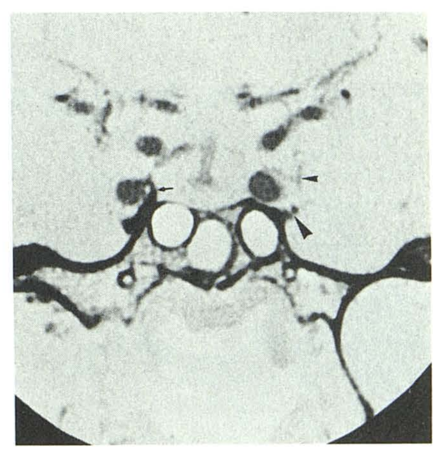

Fig. 7.—Asymmetry of venous opacification of cavernous sinuses. On right, large vein of carotid sulcus (*arrow*). On left, poorly enhanced cavernous sinus is represented by tiny inferolateral venous group (*large arrowhead*) and veins of lateral wall (*small arrowhead*). Carotid sulcus vein is absent because left intracavernous internal carotid artery is in close contact with sphenoid bone.

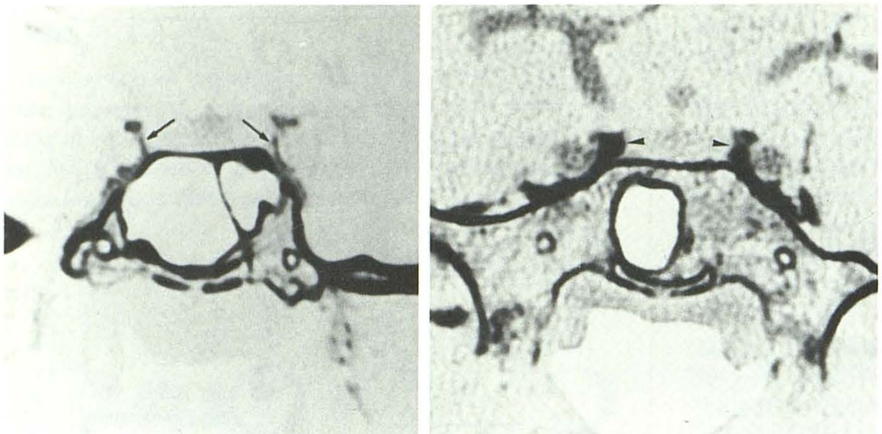

A B

Fig. 8.—*A*, Thin, symmetric medial veins bilaterally (*arrows*).

B, Thick, symmetric veins (*arrowheads*) bilaterally communicate freely with vein of carotid sulcus and inferolateral venous group.

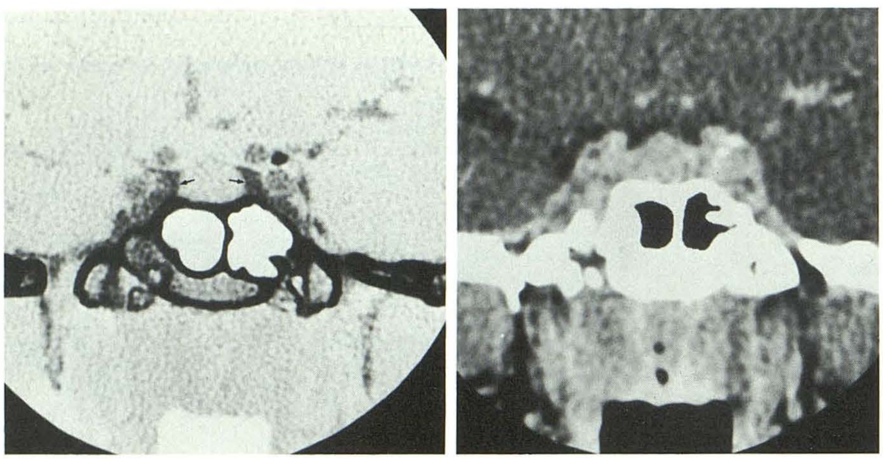

A B

Fig. 9.—*A*, Prominent bilateral medial veins (*arrows*).

B, Associated small width of sellar floor (as anatomic variant) gives rise to narrow pituitary fossa with resulting upper bulging of pituitary gland.

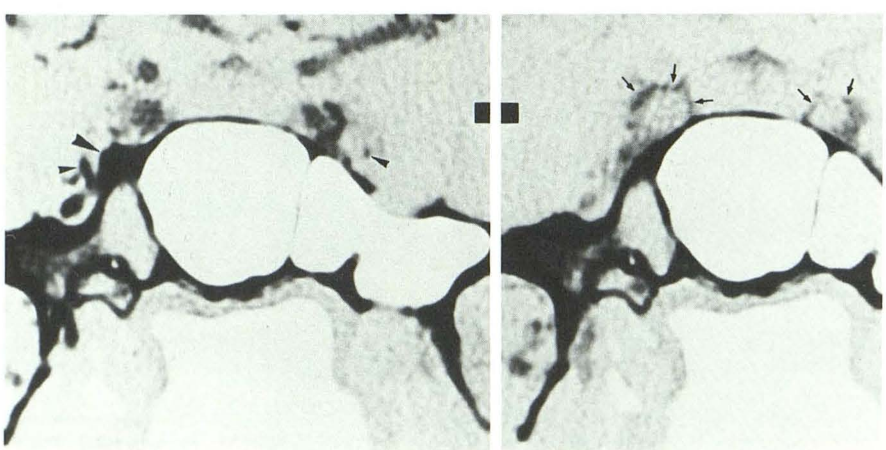

A B

Fig. 10.—Intracavernous pericarotid plexus (*arrows*) shows delayed enhancement relative to other laterosellar veins (*arrowheads*). This is due to very small size of veins of pericarotid plexus.

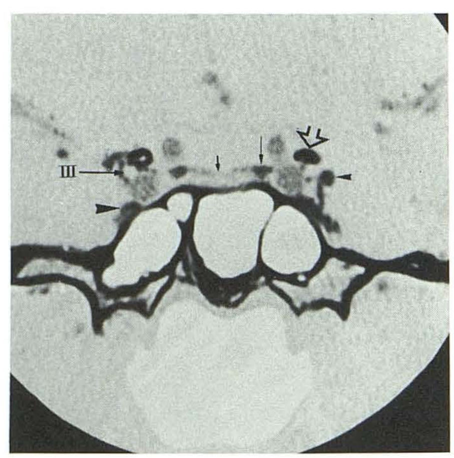

Fig. 11.—Coronal dynamic CT scan at level of anterior clinoid processes (*open arrow*) shows anterior intercavernous sinus (*short solid arrow*) with its lateral attachments (*long solid arrow*), vein of lateral wall (*small arrowhead*), inferolateral venous group (*large arrowhead*), and oculomotor nerve (III).

the internal carotid artery lies close to the lateral wall of the sphenoid sinus; that is, when there is no space between internal carotid artery and sphenoid bone. In all other anatomic situations the vein of the carotid sulcus normally is present.

Medial vein.—The medial vein appears on coronal and axial sections as a linear or comma-shaped structure delineating the border between the cavernous sinus and pituitary fossa (Fig. 8). A well-enhanced large vein is present uni- or bilaterally in 20% of cases between the intracavernous internal carotid artery and the pituitary gland; smaller and less enhanced medial veins can be demonstrated in 30% of cases. In rare cases, prominent bilateral medial veins can narrow the pituitary fossa width, giving rise to an upward bulging of the pituitary upper border (Fig. 9).

Pericarotid plexus.—Visualization of the pericarotid plexus is rare in the early venous phase. At this time, a thin lucent-free space surrounding the internal carotid artery can be present, corresponding to the internal carotid artery wall and the nonenhanced pericarotid plexus. Enhancement of the pericarotid plexus is delayed in relation to the other laterosellar veins. When present, the pericarotid plexus is thin and generally incompletely surrounds the internal carotid artery medially or laterally. In a few cases, the pericarotid plexus completely surrounds the intracavernous internal carotid artery (Fig. 10).

Intercavernous connections [16].—In our series, the *anterior* intercavernous sinus was rarely seen because of the midsellar level chosen for coronal dynamic CT. When dynamic CT is performed at the tuberculum sellae level, the anterior intercavernous sinus can be visible either completely, as a dense band extending from right to left (Fig. 11), or, more frequently, incompletely, due to its semicircular shape. In other cases, only flared lateral extremities of the anterior intercavernous sinus are demonstrated.

The *inferior* intercavernous sinus is demonstrated only when large enough, and it is seen as an enhanced band doubling the sellar floor. In some cases, the inferior intercavernous sinus is large enough to push the pituitary gland upward, resulting in a convex upper surface of the pituitary gland (Fig. 12). Demonstration of a prominent inferior intercavernous sinus can be of interest to the neurosurgeon when transsphenoidal surgery is considered.

The *posterior* intercavernous sinus is very small anatomically and we have not seen it radiologically.

The *basilar plexus*, located behind the dorsum sellae, is usually well seen in axial section.

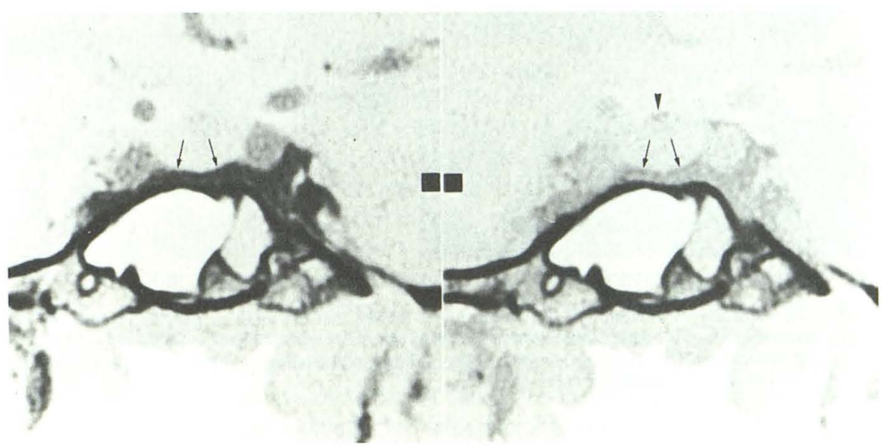

Fig. 12.—Thick inferior intercavernous sinus (*arrows*) just above and in contact with sellar floor. Slight upward displacement of pituitary capillary bed (*arrowhead*).

TABLE 1: Routine vs Dynamic CT in the Evaluation of Intracavernous Invasion by Pituitary Adenoma

Tumor Type: Case No.	Age	Gender	Routine CT: Cavernous Sinus	Dynamic CT: Carotid Sulcus Vein
Nonsecreting:				
1	64	M	Questionable on left	Not seen on left
Prolactin-secreting:				
2	48	M	Abnormal on right	Not seen on right
3	32	M	Abnormal bilaterally	Not seen bilaterally
4	48	F	Normal	Not seen on right
5	30	F	Abnormal on left	Not seen on left
Growth-hormone–secreting:				
6	32	M	Normal	Not seen on left
7	52	F	Questionable on left	Not seen on left
8	31	F	Questionable on left	Not seen on left
Growth-hormone– and prolactin-secreting:				
9	39	F	Normal	Not seen on right
10	37	M	Abnormal bilaterally	Not seen bilaterally
11	55	M	Questionable bilaterally	Not seen bilaterally
Follicle-stimulating-hormone–secreting:				
12	73	M	Abnormal bilaterally	Not seen bilaterally

Pathology

Invasion of the cavernous sinus by pituitary adenoma was diagnosed with dynamic CT in 12 patients (Table 1). There were one nonsecreting, one follicle-stimulating-hormone-secreting, four prolactin-secreting, three growth-hormone-secreting, and three mixed adenomas. Of the 12 patients, seven had undergone surgery previously or had been treated medically with bromocriptine. In five of the 12 patients, invasion of the cavernous sinus was highly suspected on the conventional CT scan when it showed bulging of the lateral wall. In seven patients, conventional CT was negative or equivocal for cavernous sinus invasion while dynamic CT was diagnostic.

The veins of the lateral wall of the cavernous sinus and the inferolateral venous group were situated too far from the pituitary fossa and were of no help in the diagnosis of cavernous sinus invasion. The medial vein, representing the true lateral border of the pituitary fossa, was never demonstrated, and because the medial vein is present in only 20–30% of normal cases, this finding was not of diagnostic value. We considered the vein of the carotid sulcus the most useful landmark. In all 12 patients the internal carotid artery was located some distance from the sphenoid sinus and the vein of the carotid sulcus was obliterated (Figs. 13 and 14). These findings constitute our earliest sign of cavernous sinus invasion. In the five patients in whom the cavernous sinus was bulging on the routine CT scan, dynamic CT demonstrated an absent carotid sulcus vein. There were no false-negative results. Surgical proof of cavernous sinus invasion was obtained in only two patients. In all other patients, only indirect proof, such as persistent abnormal hormone levels, has been

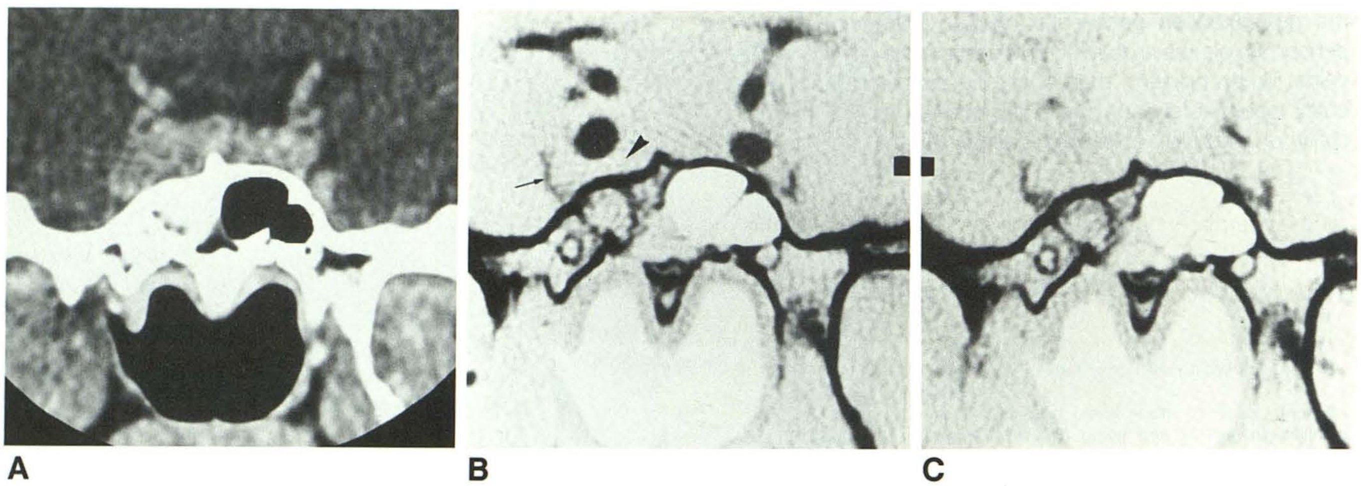

Fig. 13.—Persistent elevation of growth hormone level 6 months after surgery in 31-year-old acromegalic woman (case 8).
***A*, Routine coronal CT scan. Questionable bulging of lateral wall of cavernous sinus.**
***B* and *C*, Dynamic CT study of cavernous sinus shows obliteration of right carotid sulcus vein confirming cavernous sinus invasion (*arrowhead*). Note bowed vein of wall of cavernous sinus (*arrow*).**

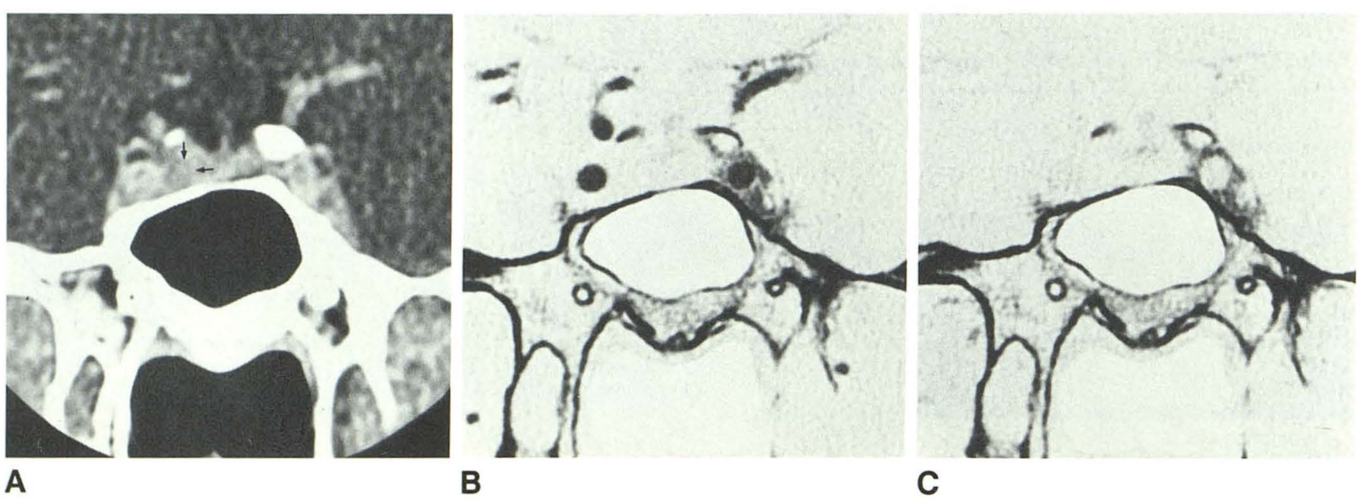

Fig. 14.—Amenorrhea-galactorrhea and hyperprolactinemia in 48-year-old woman treated with bromocriptine for 3 years (case 4).
***A*, Conventional coronal CT scan shows poorly delineated left adenoma (*arrows*).**
***B* and *C*, Dynamic CT study of cavernous sinus. Absence of carotid sulcus vein indicates cavernous sinus involvement. Cavernous sinus is well enhanced on left.**

obtained, despite complete removal of intrasellar tumoral content.

In five patients with meningiomas of the sphenoidal region, dynamic CT scanning permitted us to exclude cavernous sinus invasion by demonstrating a normal enhanced lateral wall of the cavernous sinus and normal laterosellar extradural venous spaces (Fig. 15).

Discussion

Dynamic CT scanning can routinely demonstrate the parasellar extradural venous spaces, the so-called cavernous sinus; and the same examination shows exquisitely the intracavernous cranial nerves as filling defects. There is still some controversy in the anatomic literature concerning the exact nature of the laterosellar veins. Some authors postulate that the cavernous sinus is a large channel completely surrounding the internal carotid artery. Others contend that the cavernous sinus is constituted of various-sized veins. Our study has demonstrated that the true cavernous sinus, that is, a large channel totally surrounding the internal carotid artery, is encountered in less than 1% of cases. In all other cases, the cavernous sinus is formed by numerous small veins, which can be listed as (1) the veins of the lateral wall, (2) the veins of the inferolateral group, (3) the medial vein, and (4) the vein of the carotid sulcus. The intercavernous connections can also be identified by this technique.

We postulated that since the laterosellar veins are easily demonstrated by dynamic CT and their walls are depressible, this technique could be used for demonstrating cavernous sinus invasion by pituitary tumors. Demonstrating such an invasion remains an important challenge that can modify the medical or surgical management of pituitary tumors. The ideal landmark for demonstrating cavernous sinus invasion would be the thin band of dura separating the pituitary gland from the cavernous sinus. Unfortunately, this barrier currently cannot be demonstrated routinely with either CT or MR. Careful study of the laterosellar veins now represents the best approach to determine cavernous sinus involvement.

The veins of the lateral wall of the cavernous sinus and the veins of the inferolateral group are located too far from the pituitary gland to be affected early by cavernous sinus involvement. The medial veins, situated between the pituitary gland and the internal carotid artery, are visualized inconsistently; when seen bilaterally they are of help in excluding cavernous sinus invasion. The vein of the carotid sulcus is the best radiologic landmark. This vein is more constant and is absent only when the internal carotid artery is close to the lateral wall of the sphenoid bone. Nondemonstration of the vein of the cavernous sinus in the presence of an internal carotid artery located at some distance from the sphenoid bone constitutes our best sign of early cavernous sinus invasion. Conversely, normal laterosellar extradural veins permit us to exclude cavernous sinus involvement when there is a large regional tumor, such as a large meningioma of the anterior clinoid process. Opacification of laterosellar veins on one side can be asymmetric in relation to the other side, and the late venous phase has to be examined carefully before confirming venous obliteration.

We routinely obtain dynamic coronal CT scans of the cavernous sinus at the midsellar level, that is, at the level chosen for demonstration of the pituitary tuft. In some cases, we have added to this examination other more anterior or posterior coronal sections or an axial dynamic CT scan, but these complementary examinations have rarely brought new information of diagnostic value. Today MR is considered by numerous authors to be the best way to demonstrate cavernous sinus invasion [17, 18]. For these authors, encasement of the internal carotid artery as demonstrated on MR is the best sign of cavernous sinus invasion. We believe that dynamic CT scanning is more sensitive in demonstrating the laterosellar extradural venous spaces, whose obliteration occurs before encasement of the intracavernous internal carotid artery. Owing to its better spatial resolution and dynamic capacity, CT currently is more effective than MR in demonstrating the laterosellar veins routinely. For this reason, we believe dynamic CT has to be considered first in the evaluation of suspected early cavernous sinus invasion by pituitary tumors.

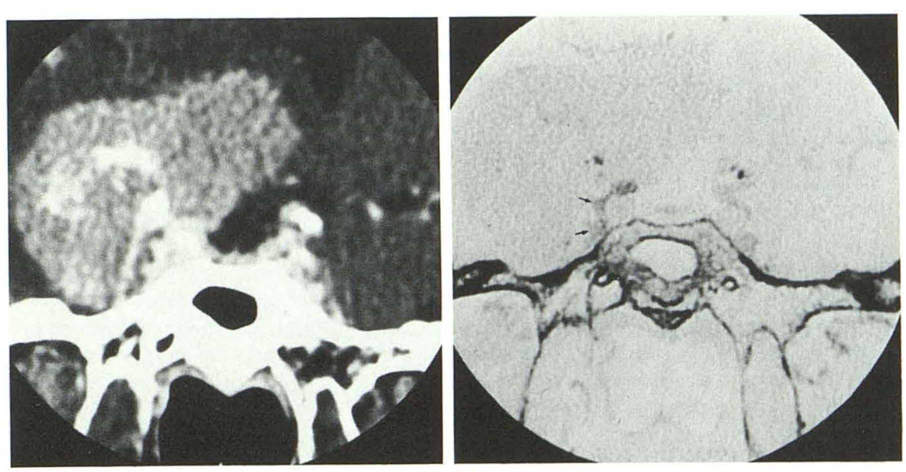

A B

Fig. 15.—Huge meningioma of right anterior clinoid process.

***A*, Routine coronal CT scan. Large suprasellar and laterosellar extension of tumor.**

***B*, Dynamic CT scan of cavernous sinus. Visualization of laterosellar extradural venous spaces (*arrows*) surrounding intracavernous internal carotid artery permits exclusion of cavernous sinus invasion.**

ACKNOWLEDGMENTS

We thank the technical staff and the secretarial staff of the Department of Neuroradiology in Besançon for their help and Michel Gaudron for photographic work.

REFERENCES

1. Olivier E, Papamiltiades M. Le système caverneux veineux de la région latérosellaire. *Bull Assoc Anat* (Nancy) **1951**;36:769–773
2. Pernkopf E. *Atlas of topographic and applied human anatomy*, vol. 1. Philadelphia: Saunders, **1963**
3. Paturet G. *Traité d'anatomie humaine*, vol. 4. *Système nerveux*. Paris: Masson, **1964**
4. Parkinson D. A surgical approach to the cavernous portion of the carotid artery. Anatomical studies and case report. *J Neurosurg* **1965**;23: 474–483
5. Harris FS, Rhoton AL. Anatomy of the cavernous sinus. A microsurgical study. *J Neurosurg* **1976**;15:169–180
6. Rhoton AL, Harris FS, Reen H. Microsurgical anatomy of the sellar region and cavernous sinus. *Neurosurgery* **1978**;8:54–58
7. Gray H. *Anatomy of the human body*, 36th ed. Edinburgh: Churchill-Livingstone, **1980**
8. Kline LB, Acker JD, Post MJD, Vitek JJ. The cavernous sinus: a computed tomographic study. *AJNR* **1981**;2:299–305
9. Taptas JN. The so-called cavernous sinus: a review of the controversy and its implications for neurosurgeons. *Neurosurgery* **1982**;11:712–717
10. Umansky F, Nathan H. The lateral wall of the cavernous sinus with special reference to the nerves related to it. *J Neurosurg* **1982**;56:228–234
11. Dolenc VV. Direct microsurgical repair of intracavernous vascular lesions. *J Neurosurg* **1983**;58:824–831
12. Rouviere H, Delmas A. *Anatomie humaine*, 12th ed. Paris: Masson, **1985**
13. Bonneville JF, Cattin F, Moussa-Bacha K, Portha C. Dynamic computed tomography of the pituitary gland: the "tuft sign." *Radiology* **1983**; 149:145–148
14. Bonneville JF, Cattin F, Dietemann JL. *Computed tomography of the pituitary gland*. Berlin: Springer-Verlag, **1986**
15. Daniels DL, Pech P, Mark L, Pojunas K, Williams AL, Haughton VM. Magnetic resonance imaging of the cavernous sinus. *AJNR* **1985**;6: 187–192
16. Kaplan HA, Browder J, Krieger AJ. Intercavernous connections of the cavernous sinuses. *J Neurosurg* **1976**;45:166–168
17. Kucharczyk W, Davis DO, Kelly WM, Sze G, Norman D, Newton TH. Pituitary adenomas: high-resolution MR imaging at 1.5 T. *Radiology* **1986**;161:761–765
18. Scotti G, Yu CY, Dillon WP, et al. MR imaging of cavernous sinus involvement by pituitary adenomas. *AJNR* **1988**;9:657–664